

**CHAPTER 5:**  
**COMPUTER SIMULATION OF THE NO<sub>x</sub> ABATEMENT PROCESS**  
**AS A KINETIC-REACTION MODEL**

## 5.1 Introduction

The equilibrium model in Chapter Four proved insufficient in its representation of the catalyst vessel. We found the simulation of that unit to be often unstable and at all times erroneous. The calculations required to implement the equilibrium assumption for the catalyst vessel caused serious problems for ASPEN.

This chapter represents our attempt to develop a working model for SCR. We resort to kinetic equations found in the literature for the important reactions occurring in the catalyst vessel. The results for the kinetic model of the catalyst vessel imitate the data provided by RFAAP and give a clearer picture of the actual process than those of any previous model.

With the work for this chapter, we arrive at a hybrid equilibrium-kinetic model that accurately and precisely simulates both the scrubber/absorber and the catalyst vessel. Chapter Six utilizes this final evolution of the ASPEN model to explore retrofit options for improving overall NO<sub>x</sub> removal performance for the NO<sub>x</sub> abatement system at RFAAP.

## 5.2 The Kinetic-Reaction Model

### 5.2.1 Motivation for a Kinetic-Reaction Absorption Model

The equilibrium model we present in Chapter 4 simulates the scrubber/absorber quite well for a variety of conditions. The results for the catalyst vessel as modeled by equilibrium reactions are less promising. In contrast to the absorber, the behavior of the catalyst vessel depends strongly on rates of reaction. Equilibrium modeling, therefore, represents an altogether inappropriate method for simulation of that unit. Also, the literature on NO<sub>x</sub> absorption is rife with justification of the equilibrium assumption for the reactions and devoid of rate data for them. On the other hand, data for the kinetics of selective catalytic reduction reactions is available in literature on the subject. Because of the failure of the equilibrium model for the catalyst vessel and the availability of kinetic data, we place a high priority on developing a kinetic model for this unit.

### 5.2.2 Mechanism of Kinetic Reactions

As we allude to above, the kinetic model is actually a kinetic-equilibrium hybrid. We use the equilibrium model for the scrubber/absorber. ASPEN determines vapor-liquid compositions and reaction conversion on the scrubber and absorber stages by equilibrium calculations. Using data from the literature, we develop a kinetic model for the catalyst vessel. Starting with the reactions in Table 5.1, we determine which of these are important under the conditions observed at RFAAP.

Table 5.1. Reactions that occur in the catalyst vessel.

Rxn. #	Reaction Stoichiometry
5.1	$4\text{NH}_3 + 6\text{NO} \leftrightarrow 5\text{N}_2 + 6\text{H}_2\text{O}$
5.2	$4\text{NH}_3 + 4\text{NO} + \text{O}_2 \leftrightarrow 4\text{N}_2 + 6\text{H}_2\text{O}$
5.3	$2\text{NO}_2 + 4\text{NH}_3 + \text{O}_2 \leftrightarrow 3\text{N}_2 + 6\text{H}_2\text{O}$
5.4	$\text{NO} + \text{NO}_2 + 2\text{NH}_3 \leftrightarrow 2\text{N}_2 + 3\text{H}_2\text{O}$

Note: These reactions are provided by RFAAP

The section on catalyst configurations in Chapter 2 discusses the role that  $\text{NH}_3$  and  $\text{O}_2$  play on the catalyst surface. In short, ammonia binds to the surface quickly, and NO bonds with the adsorbed ammonia molecule. This reaction forms nitrogen and water, and then they leave the catalyst surface. Oxygen serves to restore the catalyst surface reactivity. Though the mechanism is complex, in essence,  $\text{O}_2$  increases the rate of reaction of NO and  $\text{NH}_3$  on the catalyst surface. Therefore, in the presence of substantial oxygen, reaction (5.2) proceeds much more quickly than reaction (5.1). Willi et al. (1996) show that a total lack of  $\text{O}_2$  in the feed to a vanadia-based catalyst vessel reduces the conversion of NO almost completely. This situation corresponds to that of reaction (5.1) for the absence of oxygen. The specifications of the feed to our system give the molar fraction of oxygen as 0.2 (20,000 ppmv). The molar fraction of NO is only 0.0021 (2100 ppmv). We ignore the contribution from reaction (5.1) because of this 100-fold factor of  $\text{O}_2$ . We also use reaction (5.3) to describe

The literature suggests that the rate of reaction within the catalyst vessel is independent of ammonia partial pressure. This observation results from the extremely fast, binding reaction of ammonia to the surface of the catalyst. Therefore, surface coverage of the catalyst with ammonia molecules depends on the rate of regeneration of the catalyst surface by  $\text{O}_2$  more than on ammonia availability. Below a certain ammonia partial pressure, however, the reaction rate must decrease, and eventually approaches zero when the ammonia partial pressure approaches zero. Put simply, the reaction cannot proceed without ammonia, so some dependence on ammonia exists for the SCR reactions. We arrive at reasonable values by trial and error using the base-case inputs and outputs as known quantities.

### *5.2.3 Characteristics of the Kinetic Model*

The literature contains extensive data on the rates of reaction 5.2 over various catalyst types. Marangozis reviews the literature on the mechanism and rate parameters for NO reduction with ammonia (Marangozis, 1992). We use equation 5.5 to describe the rate of reaction 5.2.

Little information exists in the literature concerning the reactions involving  $\text{NO}_2$ , because  $\text{NO}_2$  is virtually non-existent in the stationary combustion processes for which engineers design and chiefly use SCR. In our case, the  $\text{NO}_2$  content remains very low, but is not negligible. Therefore, we determine reasonable values for the parameters in equation 5.6 by trial-and-error calculations. Table 5.2 lists descriptions and values for the parameters we use in equations 5.5 and 5.6.

$$-4d\text{NO}/dt = A_1 e^{E_1/RT} (p_{\text{NO}})^a (p_{\text{O}_2})^b (p_{\text{NH}_3})^c \quad (5.5)$$

$$-2d\text{NO}_2/dt = A_2 e^{E_2/RT} (p_{\text{NO}_2})^x (p_{\text{O}_2})^y (p_{\text{NH}_3})^z \quad (5.6)$$

Table 5.2. Parameter values for the reduction of NO and NO<sub>2</sub> with ammonia.

Symbol	Description	Units	Value	Source
A <sub>1</sub>	Pre-exponential (eq. 5.5)	kg-mol/(sec*m <sup>3</sup> )	15E6	Willi et al. (1996)
E <sub>1</sub>	Activation energy (eq. 5.5)	kcal/g-mol	15	Marangozis (1992)
R	Gas constant	Psia/lbmol-°R	10.73	
A	Order with respect to NO	Unitless	1	Marangozis
B	Order with respect to O <sub>2</sub>	Unitless	0.5	Marangozis
C	Order with respect to NH <sub>3</sub>	Unitless	0.0005	
p <sub>NO</sub>	NO partial pressure	psi	*	
p <sub>O2</sub>	O <sub>2</sub> partial pressure	psi	*	
p <sub>NO2</sub>	NO <sub>2</sub> partial pressure	psi	*	
p <sub>NH3</sub>	NH <sub>3</sub> partial pressure	psi	*	
A <sub>2</sub>	Pre-exponential (eq. 5.6)	kg-mol/(sec*m <sup>3</sup> )	15E6	
E <sub>2</sub>	Activation energy (eq. 5.6)	kcal/g-mol	14.5	
Y	Order with respect to NO <sub>2</sub>	Unitless	1	
Z	Order with respect to O <sub>2</sub>	Unitless	0.5	
C	Order with respect to NH <sub>3</sub>	Unitless	0.0005	

\* Denotes that the value varies depending on feed and catalyst-vessel operating conditions.

A simple kinetic reaction takes account of the effect of water on the SCR reactions as described by Willi et al. (1996). We represent the effect of water simply as the reverse of reaction 5.2. We determine reaction-rate parameters from trial and error that gives comparable effects to those found in the literature. We present the rate equation for the reverse of reaction 5.2 in equation 5.7 below. Table 5.3 summarizes the parameter values we use in equation 5.7.

$$+4dNO/dt = A_3 e^{E_3/RT} (p_{H_2O})^d (p_{N_2})^e \quad (5.7)$$

Table 5.3. Parameter values in rate equation 5.7 for the reverse of reaction 5.2.

Symbol	Description	Units	Value
A <sub>3</sub>	Pre-exponential (eq. 5.7)	kg-mol/(sec*m <sup>3</sup> )	0.1
E <sub>3</sub>	Activation energy (eq. 5.7)	kcal/g-mol	10
R	Gas constant	Psia/lbmol-°R	10.73
d	Order with respect to N <sub>2</sub>	Unitless	0
e	Order with respect to H <sub>2</sub> O	Unitless	0.3
p <sub>H2O</sub>	H <sub>2</sub> O partial pressure	Psi	Variable
P <sub>N2</sub>	N <sub>2</sub> partial pressure	Psi	Variable

We next need information on the construction of the catalyst vessel. We assume that the catalyst vessel operates as a simple plug-flow reactor for the purposes of our model. From information provided by personnel at RFAAP, we determine the volume and residence time of the reactor. Table 5.4 lists the pertinent values.

Table 5.4. Values concerning physical aspects of the catalyst vessel.

Number of catalyst modules	8
Catalyst module dimensions, ft	4 x 3 x 2
Void-volume fraction of catalyst module, ft <sup>3</sup> void / ft <sup>3</sup> total	0.725
Void volume of catalyst vessel, ft <sup>3</sup>	139.2
Volumetric flow rate of fumes, ft <sup>3</sup> /min	9000 (approx.)
Residence time of fumes, min (sec)	0.015 (0.9)

The void-volume fraction represents the ratio of the catalyst-bed free volume to total volume. In other words, this value equals the open fraction of the catalyst vessel not filled with solid catalyst. We calculate the void volume of the catalyst as the volume open to gas flow. We use this volume to calculate the residence time of the gas. ASPEN Plus uses the data in Table 5.4 to calculate the reaction conversions from the rates and residence time assuming perfect radial mixing.

### 5.3 Discussion of the Kinetic Model

#### 5.3.1 Results of the Kinetic Model

Table 5.5 gives the results of the kinetic model for key streams. We also show the results for these streams from the equilibrium model as well as those provided by RFAAP for comparison. As the reader can see, a close agreement exists between the different sets of results.

Table 5.5. Stream results for the kinetic model as compared to previous results.

Stream: Mole Flow Lbmol/hr	PRODUCT (Kinetic Model)	PRODUCT (Equilibrium Model)	PRODUCT (Conversion Model)	Gas to Vent Stack (RFAAP Data)
NO	0.27	0.22	0.06	0.06
NO <sub>2</sub>	0.044	0.035	9.7E-3	trace
NH <sub>3</sub>	0.081206	0	0	trace
O <sub>2</sub>	132	132	132.1	132.06
N <sub>2</sub>	498.9	498.7	498.8	496.8
H <sub>2</sub> O	23.0	23.5	15.9	23.9
HNO <sub>2</sub>	0	-	-	-
HNO <sub>3</sub>	0	-	-	-
Total Flow lbmol/hr	654.0	654.4	646.8	654.8
Total Flow lb/hr	18618	18624	18487	18631
Temperature F	350	350	350	350
Pressure psi	15	14.9	14.4	14.1

Note: The kinetic model required 1.9 lbmol/hr NH<sub>3</sub> feed to the SCR for these results.

### 5.3.2 Sensitivity Analysis

The scrubber/absorber model remains identical to that found in Chapter 4. Therefore, the sensitivity simulations we present for the kinetic model encompass only the catalyst vessel. We consider several factors that could be affected by the upstream flow from the scrubber/absorber. The two processes operate relatively independent of each other. However, the output from the scrubber/absorber represents the input to the catalyst vessel, so we require some accounting for this situation.

#### 5.3.2.1 NO Flow Rate to Catalyst Vessel

At constant  $\text{NH}_3$  to NO molar feed ratio to the catalyst vessel, we vary the NO flow rate. We expect the amount of NO escaping the catalyst vessel to be constant because the residence time for the catalyst vessel remains the same. However, the reaction rate depends on the concentration of NO as well. Thus, the higher NO concentration due to the constant inert flow rate should increase the overall fractional conversion of NO. We show the effect of NO feed rate on NO and  $\text{NO}_2$  fractional conversion in Figure 5.1. Figure 5.2 shows the effect on the molar flow rate of NO escaping the catalyst vessel.

Figure 5.1 shows that the fractional conversions of both NO and  $\text{NO}_2$  indeed increase for an increase in NO. The increased conversion of  $\text{NO}_2$  results from the requisite increase in ammonia feed rate to keep the  $\text{NH}_3$ -to-NO molar feed ratio constant. The efficiency of the catalyst vessel increases with increasing NO concentration as Figure 5.1 shows. However, as we see in Figure 5.1 the rate of NO escape from the reactor increases as well.

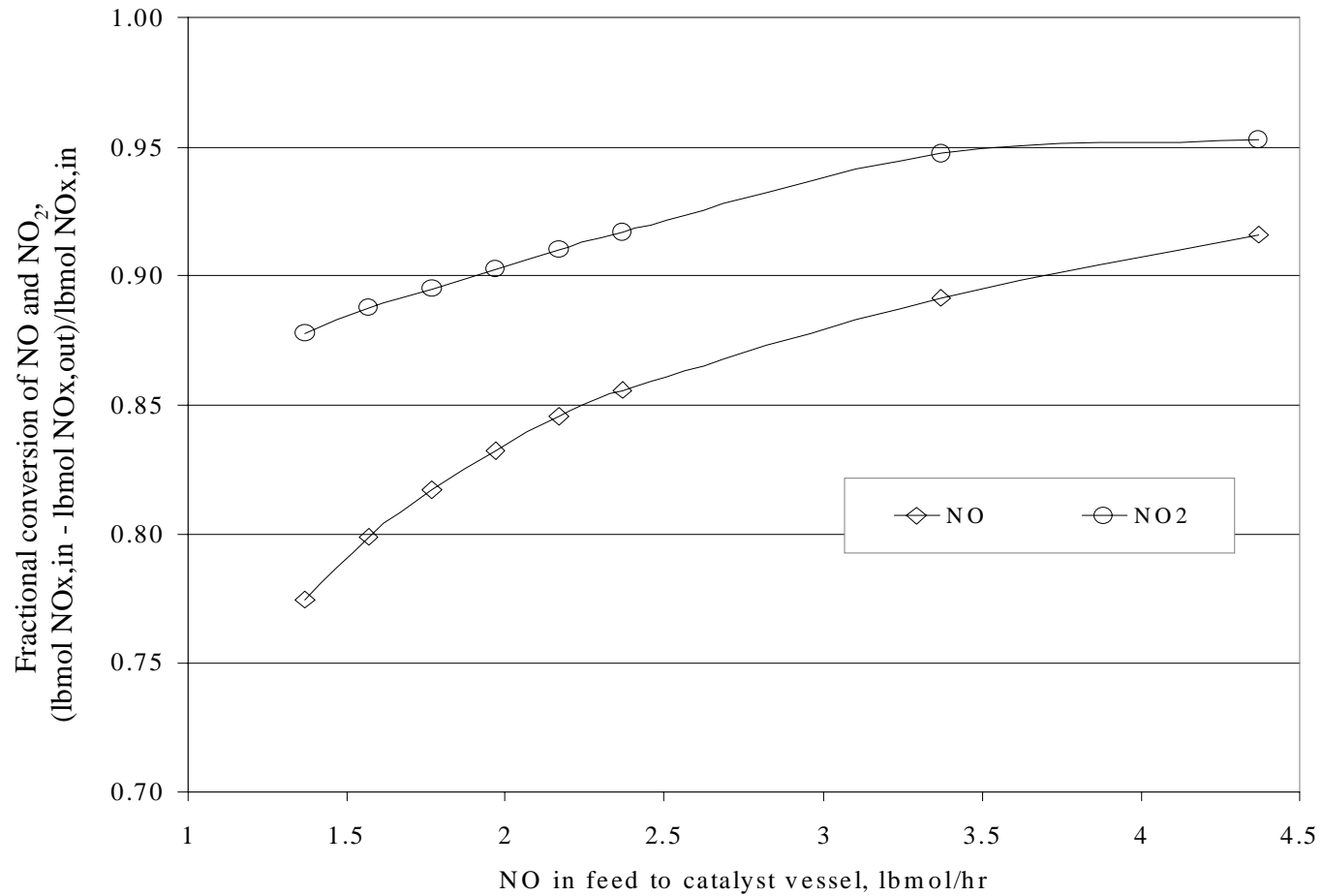


Figure 5.1. Plot of fractional conversions of NO and NO<sub>2</sub> versus the feed rate of NO to the catalyst vessel.

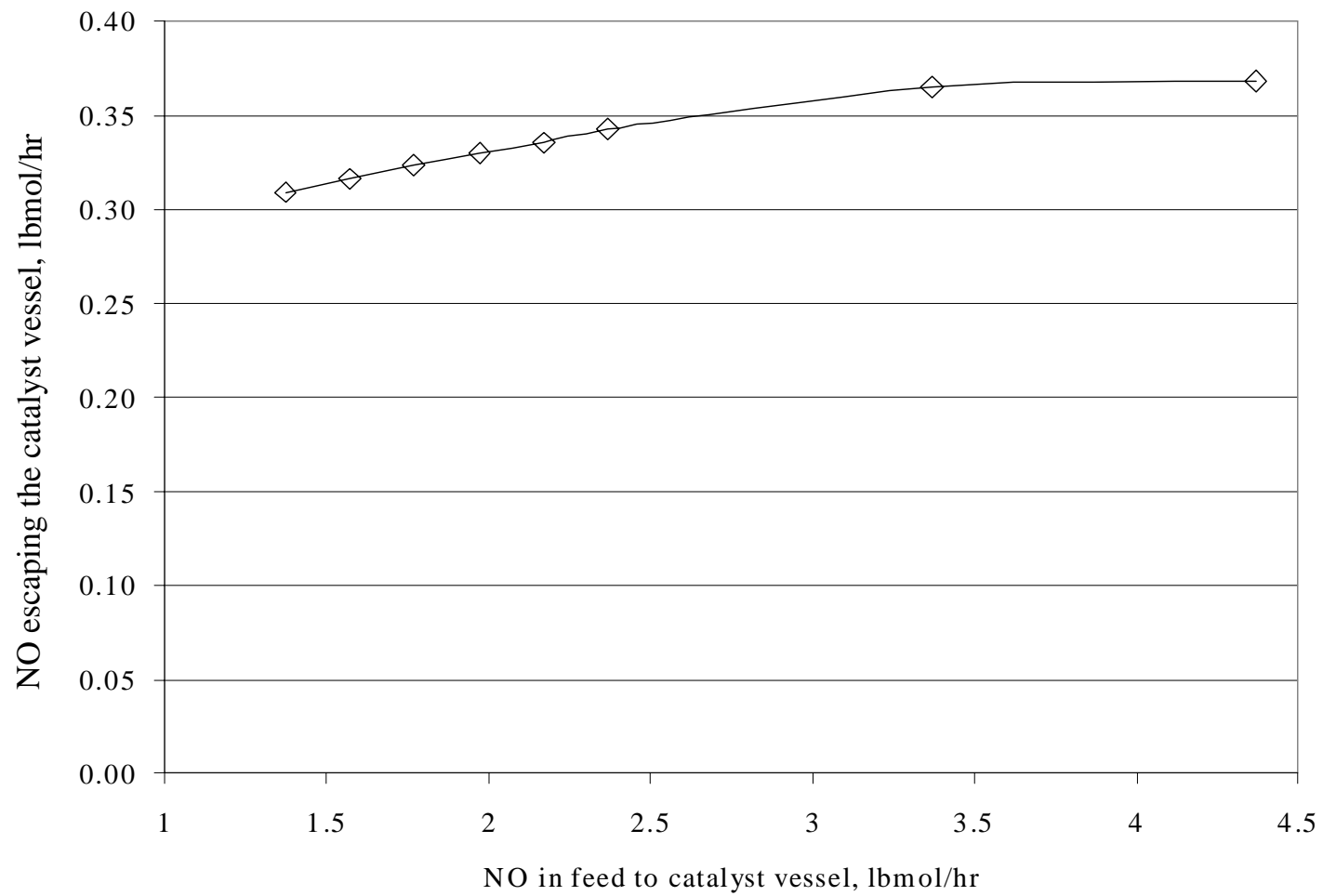


Figure 5.2. Plot of NO escaping the catalyst vessel versus the feed rate of NO to the catalyst vessel.

### *5.3.2.2 Ammonia Flow Rate to Catalyst Vessel*

The literature states that SCR is extremely sensitive to the ammonia feed. An optimum exists for the feed ratio of NO<sub>x</sub> to ammonia entering the catalyst vessel. This optimum maximizes the conversion of NO<sub>x</sub>, while minimizing the ammonia slip. We vary the ammonia flow to the catalyst vessel for constant NO<sub>x</sub> feed rate to determine this optimum value in Figure 5.3.

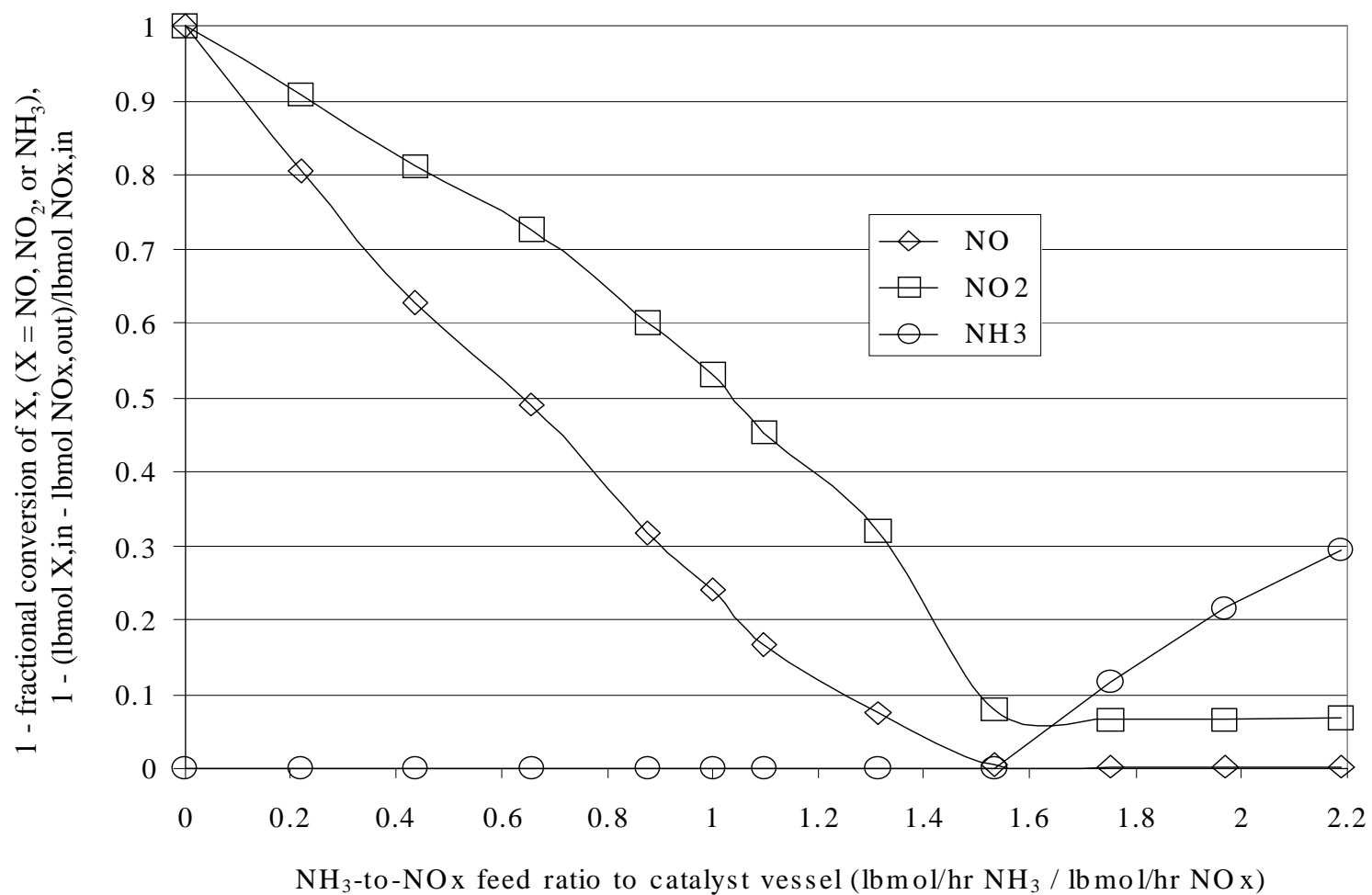


Figure 5.3. Plot of the fraction of the feed that escapes the catalyst vessel versus the ammonia to NO<sub>x</sub> feed ratio.

### 5.3.2.3 *Steam Flow Rate to Catalyst Vessel*

Willi et al. (1996) state that the water in the feed to SCR negatively affects the reaction rate over vanadia-based catalyst beds. Their experiments show that water concentrations of up to 2.5% by mole (25,000 ppmv) reduce the conversion of NO by approximately 10% or more. Above 2.5% water, the reduction in reaction conversion remains but does not increase. The gas exiting the scrubber/absorber for the base case results contains approximately 3.3% (33,000 ppmv) water. The addition of 21 lb/hr of steam to vaporize the ammonia feed brings the water content of the catalyst vessel feed to approximately 3.5% (35,000 ppmv). This value is well above the value that Willi et al. found to produce the greatest reduction in catalyst vessel performance.

The result that we expect from the model is slightly different from those in the results from Willi et al. In the actual catalytic process, water inhibits the regeneration of active catalyst surface sites. Therefore, because water participates in a surface interaction on the catalyst after a certain concentration (2.5% or 25,000 ppmv in this case), additional water in the feed does not have any effect on the fractional conversion. Because we have added a rate for the reverse of reaction 5.2 in our model, the negative effect of water continues to rise as we add more water in the feed. Figure 5.4 shows the results for the effect of water in the catalyst vessel as compared to those of Willi et al.

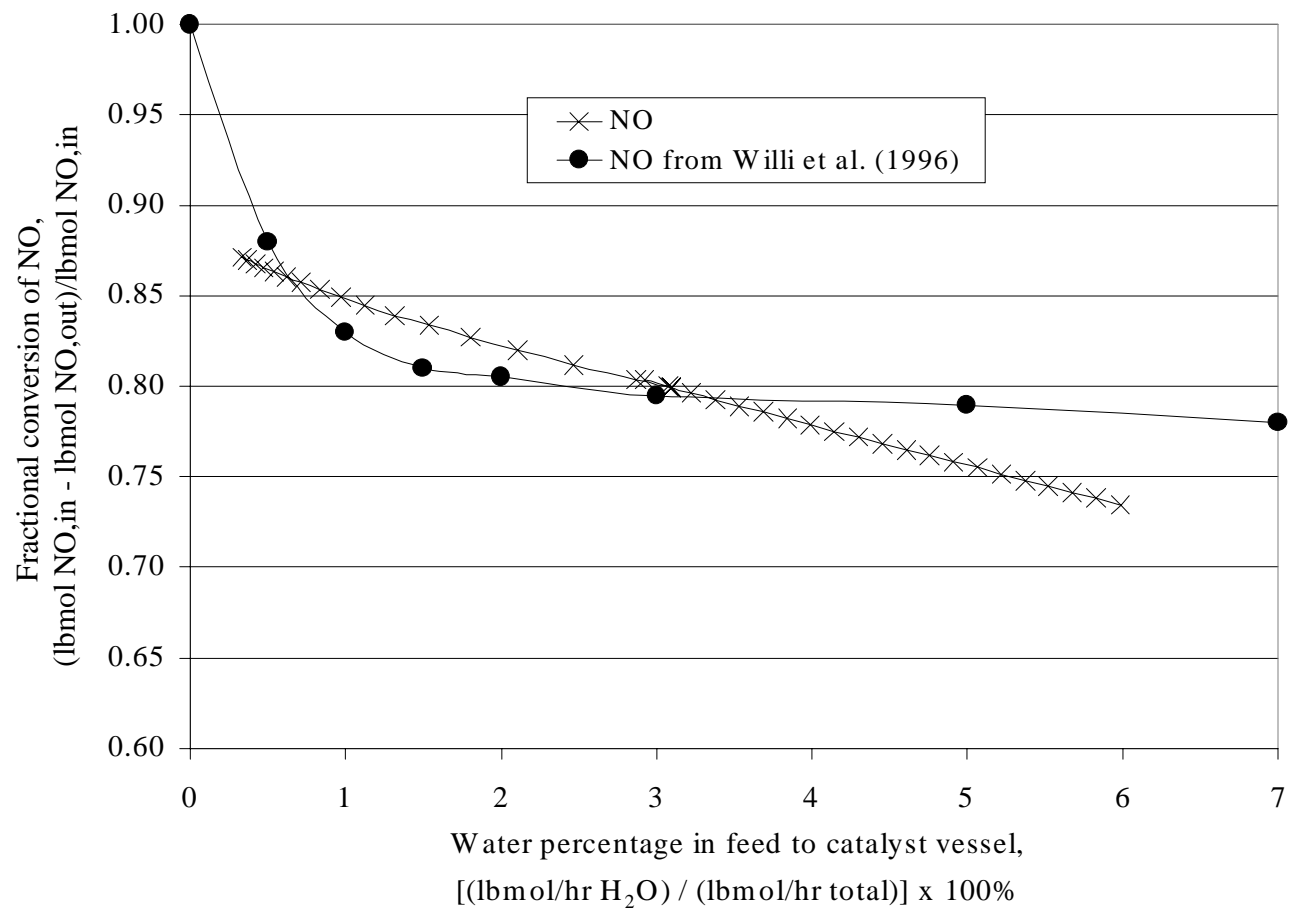


Figure 5.4. Plot of the effect of water in the feed on the fractional conversion of NO. We present our model results for comparison to those of Willi et al. (1996).

#### 5.3.2.4 *Oxygen Percentage in Feed to Catalyst Vessel*

As we state previously, oxygen profoundly affects the performance of the catalyst vessel. Willi et al. (1996) presents data showing that lack of oxygen virtually halts NO reduction. The system at RFAAP feeds oxygen in great excess; however, we must consider this important effect. Figure 5.5 shows results of the ASPEN Plus simulation for wet and dry feed to the catalyst vessel as well as results presented by Willi et al.

The results from the kinetic model simulation agree well with the results presented by Willi et al. although giving slightly lower conversion fractions. However, we can attribute most of this disagreement to differences in the system they investigate. For example, oxygen feeds to the catalyst vessel at RFAAP at approximately 20%. The difficulties with modeling the effect of oxygen arise from the complex interaction of oxygen with the catalyst surface. At approximately 11% oxygen in the feed, Willi et al. observe a maximal surface coverage of oxygen on the catalyst. Our model uses a simple rate expression for oxygen that cannot identically match such a dramatic asymptote as Willi et al. observe. Still, the results for our model satisfy the system at higher oxygen partial pressures appropriate to this system. Figure 5.5 also reiterates the effect of water in the feed. An addition of 3.3% water to the feed stream dramatically shifts the curves for the conversion of NO down. Obviously, we should minimize the water feed to the catalyst vessel and keep the oxygen feed percentage above 10% for maximal conversion of NO.

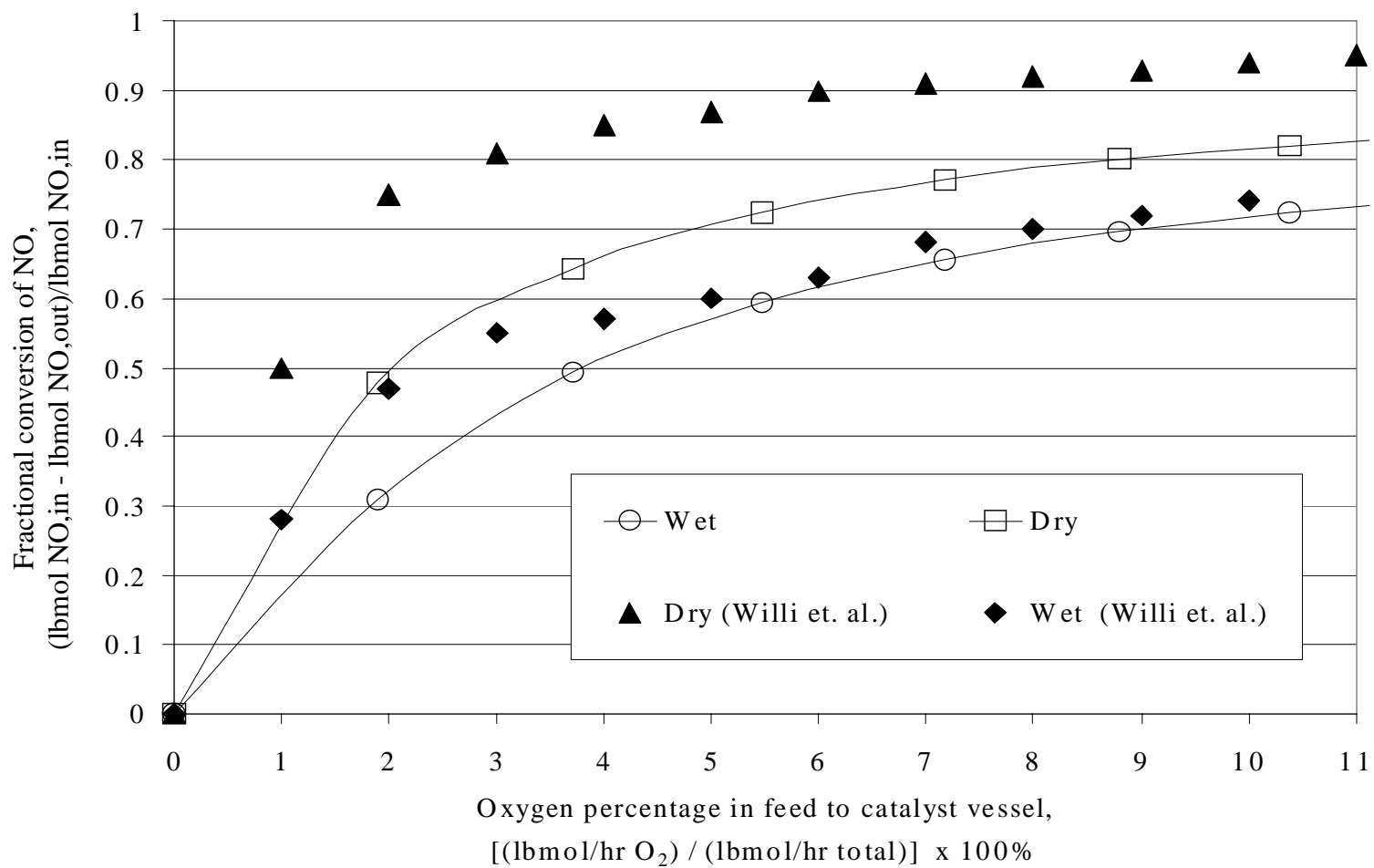


Figure 5.5. Plot of the effect of oxygen in the feed on the fractional conversion of NO. We present our model results for comparison to those of Willi et al. (1996).

### 5.3.2.5 *Pressure of Catalyst Vessel Feed*

Gas-phase reactions depend strongly on pressure. We desire to determine the effect of pressure on the SCR reactions. Recall that pressurizing the scrubber/absorber improves the performance of that unit. Improvement of the catalyst vessel performance would strengthen the case for such a measure. Figure 5.6 shows results for NO and NO<sub>2</sub> conversion in the catalyst vessel for increasing pressure for both dry and wet feeds (0.15 and 3.5 percent moisture in feed respectively).

Increasing the pressure of the catalyst vessel feed induces a clear improvement in both NO and NO<sub>2</sub> conversion. Diminishing returns set in between 25 and 30 psia for the removal of both components. Pressures above 25 psia ensure nearly complete removal of NO<sub>2</sub>. The simulation shows little effect of water in the feed on NO<sub>2</sub> conversion, although the effect on NO is great. However, the negative effect of water decreases markedly at higher pressures to where it is almost nonexistent at 30 psia.

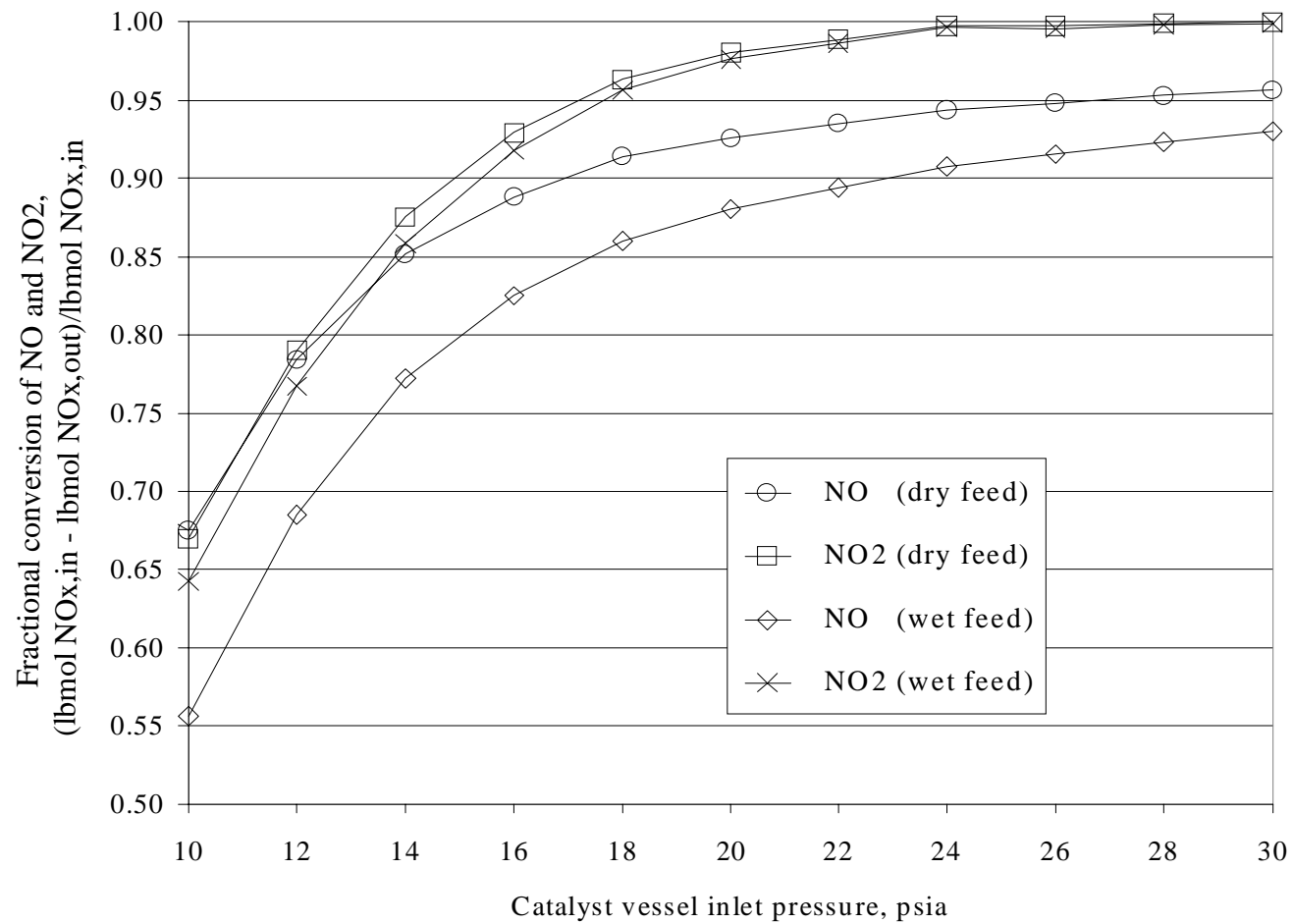


Figure 5.6. The effect of pressure and moisture in the feed on the fractional conversions of NO and NO<sub>2</sub>.

## 5.4 Conclusions

1. Increasing the NO feed concentration to the catalyst vessel by 300 percent, while maintaining a constant NH<sub>3</sub>-to-NO<sub>x</sub> ratio, increases the NO fractional conversion from 0.78 to 0.92 and the NO<sub>2</sub> fractional conversion from 0.88 to 0.95.

2. The optimum NO<sub>x</sub> removal, while, at the same time, minimizing ammonia slip, exists at a NH<sub>3</sub>-to-NO<sub>x</sub> molar ratio of 1.6. Ammonia slip rises substantially after this value, whereas further NO<sub>x</sub> reduction remains minimal.

3. The effect of water on the conversion of NO for the kinetic model differs systematically from that presented by Willi et al. (1996). The kinetic model does, however, give the same magnitude of effect as the data by Willi et al.

4. Willi et al. show that up to 2.5 percent water in the feed reduces NO conversion by 20 percent. They observe no further reduction for water levels above 2.5 percent.

5. The kinetic model simulation results agree with those of Willi et al. for the effect of oxygen on the SCR reactions. Below 11 percent of the feed, oxygen exhibits a profound effect on catalyst vessel activity. The removal of NO and NO<sub>2</sub> decreases virtually to zero for feeds devoid of oxygen.

6. Below 30 psia, increasing catalyst vessel pressure enhances NO and NO<sub>2</sub> removal for both wet and dry feeds. Increasing catalyst vessel feed pressure from 10 psia to 30 psia increases the fractional conversion of NO from 0.67 to 0.96 with all other factors (NO<sub>x</sub> molar concentrations, NH<sub>3</sub> feed rate, etc.) constant.

## 5.5 Recommendations

1. Feed NO<sub>x</sub> to the catalyst vessel in as undiluted form as is possible and appropriate.
2. For a NO-to-NO<sub>2</sub> molar feed ratio of 3.25, feed NH<sub>3</sub> to the catalyst vessel in a NH<sub>3</sub>-to-NO<sub>x</sub> molar feed ratio of 1.6.
3. Water has a negative effect on the conversion of NO over vanadia-on-titania catalyst surfaces.
4. If the water level in the feed to the SCR can be decreased below 2.5 percent, make attempts to decrease it further. If however, the feed cannot be decreased to below 2.5 percent, little benefit exists from efforts that decrease it to above this value. This conclusion arises from research in the literature and was not explicitly supported by our simulation results.
5. Keep oxygen levels in the SCR above 11 percent (by mole) at a minimum. A value of 15 percent represents a reasonable safety factor.
6. Maximize the feed and operational pressure of the catalyst vessel for improved performance.

## 5.6 Nomenclature

A <sub>1</sub>	pre-exponential	[=]	kg-mol/(sec*m <sup>3</sup> )
E <sub>1</sub>	activation energy	[=]	kcal/g-mol
R	ideal gas constant	[=]	Psia/lbmol-°R
A	reaction order with respect to NO	[=]	Unitless
B	reaction order with respect to O <sub>2</sub>	[=]	Unitless
C	reaction order with respect to NH <sub>3</sub>	[=]	Unitless
p <sub>NO</sub>	NO partial pressure	[=]	psi
p <sub>O2</sub>	O <sub>2</sub> partial pressure	[=]	psi
p <sub>NO2</sub>	NO <sub>2</sub> partial pressure	[=]	psi
p <sub>NH3</sub>	NH <sub>3</sub> partial pressure	[=]	psi
Y	order with respect to NO <sub>2</sub>	[=]	Unitless
Z	order with respect to O <sub>2</sub>	[=]	Unitless
C	order with respect to NH <sub>3</sub>	[=]	Unitless

## 5.7 References

Marangozis, J., “Comparison and Analysis of Intrinsic Kinetics and Effectiveness Factors for the Catalytic Reduction of NO with Ammonia in the Presence of Oxygen,” *Industrial Engineering and Chemistry Research*, **31**, 987 (1992).

Willi, R., B. Roduit, R. A. Koepfel, A. Wokaun, and A. Baiker, “Selective Reduction of NO by NH<sub>3</sub> Over Vanadia-Based Commercial Catalyst: Parametric Sensitivity and Kinetic Modeling,” *Chemical Engineering Science*, **51**, 2897 (1996).